

The doubly inelastic contribution to electron loss: H^0 and He^0 ($0.5 \text{ MeV } u^{-1}$) in collision with Ar

M Kuzel[†], O Heil^{†||}, R Maier[†], M W Lucas[‡], D H Jakuba[§]-Amundsen[§],
B W Farmery[‡] and K O Groeneveld[†]

[†] Institut für Kernphysik der J W Goethe Universität Frankfurt, August-Euler-Str 6, 6000 Frankfurt/Main, Federal Republic of Germany

[‡] School of Mathematical and Physical Sciences, University of Sussex, Brighton BN1 9QH, UK

[§] Sektion Physik, Universität München, Am Coulombwall 1, 8046 Garching, Federal Republic of Germany

Received 2 October 1991

Abstract. We have measured absolute doubly differential cross sections for electron loss from the simple structured projectiles H^0 and He^0 in collision with Ar. By counting electrons in coincidence with the individual charge states of the transmitted beam we are able to separate the contributions from projectile ionization and target ionization, thereby showing the importance of events where both projectile and target are ionized in a single collision: the 'doubly inelastic' events. We should like to draw attention to two possible mechanisms within the doubly inelastic channel and give a theoretical description of the dominant one, making a second Born evaluation and including it within the electron impact approximation. This can result in some overprediction of the absolute cross sections. Better numerical agreement is often achieved by calculating only the singly inelastic contribution but our experiments show that such a model is not conceptually correct.

1. Introduction

The redistribution of electrons among the many available energy levels, including those of the continuum, during an atomic collision is a fundamental process of physics. Although primarily, and rightly, seen as a problem in atomic physics it has wide consequences in other branches of physics because of its application to such diverse phenomena as aurorae, stopping power, and structural and biological aspects of radiation damage. Partly because of these wider connotations, but also from a straightforward desire to understand such a basic process, this topic has attracted the attention of many physicists since the early work of Thomas (1927), Bethe (1930) and Bohr (1948). Such early work was often concerned with total cross sections for excitation and ionization but following the revival of interest in atomic collisions in the 1960s experimenters soon learned that studies of the energy and angular distributions of ejected electrons, the doubly differential cross sections (DDCS), would provide a much

^{||} Permanent address: Lahmeyer International, Frankfurt/Main, Federal Republic of Germany.

more sensitive test of available theory. Indeed, these studies continue to provide the steady source of data needed to promote that interaction with theory so essential to a proper understanding of the mechanisms involved.

The simplest situation one can envisage is that of single ionization caused by a fast ($v \gg Z_T/n$) bare ion incident on atomic hydrogen or other low- Z_T target for which the electronic wavefunctions, of principal quantum number n , are exact or well known. For such direct ionization the first order Born approximation (Merzbacher and Lewis 1958) gives good values of the DDCS, with the notable exception of the cusp structure in the forward direction which requires special treatment (Macek 1970, Dettmann *et al* 1974).

However, the case is more complicated when the projectile carries its own electrons into the collision. Experimental measurements of the DDCS with such structured projectiles are probably as numerous as those using bare ions, but the challenge for the theory is clearly much more severe. Although we commonly speak of electron loss, meaning projectile ionization, it is clear that electrons may now originate from projectile or target and either or both may be left in an excited state. In the first experiments of this type Burch *et al* (1973) discovered a broad 'electron loss peak' which they correctly attributed to ionization of the projectile. Their semiclassical binary encounter model proposed that projectile electrons were elastically scattered by the target in a way closely resembling the scattering of free electrons (Bohr 1948). Hartley and Walters (1987b) have pointed out that the singly differential cross section for the elastic scattering of free electrons and for Burch's elastic scattering model (ESM) both show similar structure in the angular dependence (Duncan and Menendez 1979, 1981, Heil *et al* 1991d); this structure arising from the ability of the projectile electrons to probe successive shells of the target. It is particularly easy to see the operation of the ESM for 180° scattering. If a beam of free electrons with unique velocity v is incident on a heavy target, those making head-on collisions with the massive nucleus will simply bounce back at $-v$ and so display a delta-function peak at energy $v^2/2$. Since the incoming electrons actually have a velocity distribution characteristic of their initial bound state to the projectile, the delta-function changes to a broad peak characteristic of the Compton profile of that initial state. The electron loss peak may therefore be used to gain information about the initial binding of the electron to the projectile (Strong and Lucas 1977).

Quantum mechanical calculations for electron loss again started from the first Born approximation (Bates and Griffing 1954), Drepper and Briggs (1976) making the connection with target ionization by formulating the cross section in the projectile frame before transforming to the laboratory frame. This procedure immediately shows the importance of the soft collisions in producing another cusp-shaped structure at very small angles, this time characteristic of electron loss to continuum projectile states (Rudd and Macek 1972). Detailed studies of the asymmetries of these electron loss cusps now make it clear that something better than first Born is needed to describe projectile ionization, especially for heavy targets (Hartley and Walters 1987b, Jakubaßa-Amundsen 1990).

A major step forward in measurement techniques was made by DuBois and Manson (1986) who introduced coincident techniques to the data gathering. The DDCS was measured in coincidence with the charge state of the transmitted projectile so that for the first time projectile ionization and target ionization could be separated. This at last removes one of the major difficulties that plagued earlier interpretations. We still have the problem that we do not know the final state of the target but the collision is almost as well specified as for the bare projectile. The most interesting feature to emerge from

DuBois and Manson's results was a large contribution to electron ejection from collisions in which both target and projectile became *simultaneously* ionized.

In formulating an improved model for projectile ionization we must first draw attention to a distinction made by Bates and Griffing (1954). Since, for a light projectile, the amount of momentum required to eject an electron from the projectile and the amount required to excite the target are similar we see that two independent channels can contribute. In singly inelastic (SI) collisions only the projectile is ionized: the target is assumed to remain in its ground state. However when the projectile ionization is accompanied by ionization or excitation of the target the collision is inelastic with respect to both partners and so known as doubly inelastic (DI). Now we can, in fact, envisage two DI mechanisms by which simultaneous ionization might take place. Electrons from the projectile may interact directly with electrons of the target causing 'coherent projectile ionization'; alternatively a projectile electron may scatter from the target nucleus and at the same time (meaning in the same collision) an electron from the target may scatter from the projectile nucleus causing 'incoherent projectile ionization'. This second process, not included in the conventional description, is similar to two simultaneous SI processes each centred on a different nucleus. We note that Feagin *et al* (1984) were able to give an improved description of transfer excitation based on a mechanism which is similar to these two DI processes.

For our theoretical description of electron loss we use a quantum mechanical version of the ESM: the electron impact approximation (EIA). In contrast to the Born approximation or the impulse approximation of Hartley and Walters (1987b), the emitted electron is described by a scattering eigenstate of the target field. Since the influence of the projectile field on the final electronic state is neglected the forward cusp cannot be reproduced, however the prescription should be adequate for heavy targets and emission angles $\geq 30^\circ$. While the EIA theory containing only the SI contribution (Jakubařa 1980) gave a partly satisfactory description of the loss spectra from non-coincidence experiments (Kövr *et al* 1988) it failed for those coincidence experiments examining backward emission from heavy targets (DuBois and Manson 1990, Heil *et al* 1991a). Wang *et al* (1991), prompted by an unresolved discrepancy between the measured singly differential cross section for electron loss at backward angles and the theory of Hartley and Walters (1987b), have given an improved treatment of the singly inelastic contribution to EIA. This explicitly deals with the signal in the neighbourhood of the electron loss peak. However, recognizing that even such an improved SI calculation does not reproduce the experimental ejection at energies below the loss peak, the same authors point to the necessity of including the DI contribution and give an independent second-order estimate of the coherent DI mechanism for the $H^0 + Ar$ system (Wang *et al* 1992). The sum of their SI and DI channels gives good agreement with our data for $\Theta_f = 180^\circ$.

In the present work the incoherent part of the doubly inelastic process is included in the EIA theory in the framework of a second Born approach and it is shown that the incoherent projectile-target ionization gives the dominant contribution to electron loss at energies below the loss peak. We compare the EIA model with coincidence DDCS measurements of electron loss from H^0 and He^0 in collision with Ar targets. These measurements are an extension of earlier coincidence experiments using He targets (Heil *et al* 1991b).

The paper is organized as follows. Section 2 gives a description of the experiment. In section 3 the EIA theory is developed, and then the experimental spectra are compared with theory (section 4). The conclusion is drawn in section 5. Atomic units are used unless otherwise indicated.

2. Apparatus and techniques

We obtained experimental DDCs for electron emission by intersecting a high velocity neutral particle beam (H^0 , He^0) with an argon target at the entrance focus of a cylindrical mirror electron spectrometer. Electrons were observed at emission angles from 30° – 180° and with energies between 25 and 1500 eV. Additionally, the charge states (e.g. H^+ , He^+ , He^{2+}) of the transmitted projectiles were separated and counted in coincidence with the emitted electrons using a 'list mode' technique. A detailed description of the apparatus and electronics is given in Heil *et al* (1991b) and is shown here in figure 1.

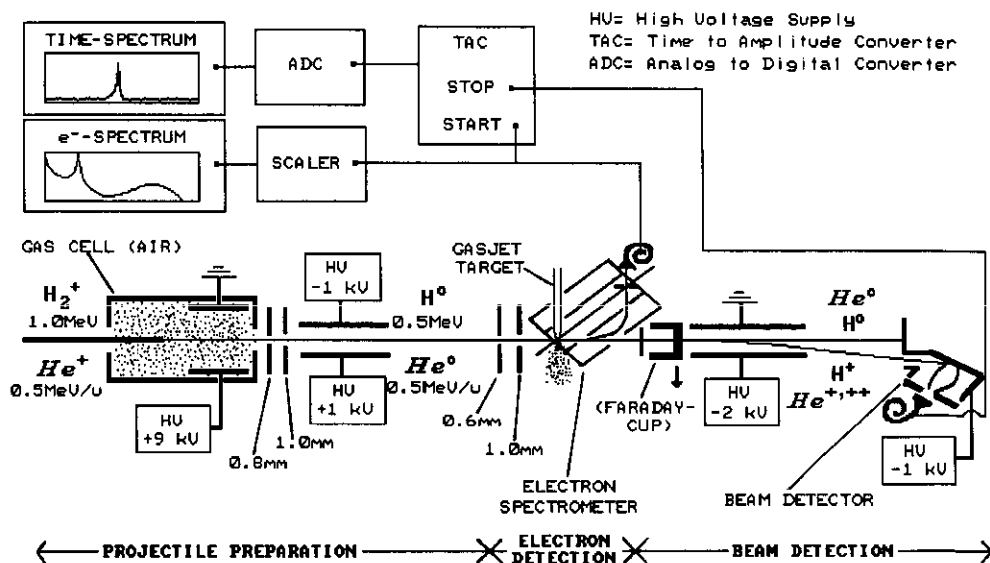


Figure 1. Schematic view of experimental apparatus.

A considerable part of our attention was directed towards the production of the neutral projectile beams; particularly removal of charged components and attempts to quench the long lived metastable states. The neutral 0.5 MeV hydrogen beam was created by dissociating molecules of momentum analysed 1.0 MeV H_2^+ in a one metre long gas cell containing ~ 0.05 mbar of air. The remaining charged components were then deflected out of the neutral beam by an electric field of 10^5 $V\ m^{-1}$ produced by electrodes at ± 1 kV potential and 0.5 m long. This electric field is sufficient to mix the 2s and 2p states of atomic hydrogen and since, at our velocity, the beam spends approximately five hundred times the lifetime of the 2p state in this field we do not expect significant contamination by the 2s or other excited states (Bethe and Salpeter 1957). Production of the neutral helium beam was achieved by electron capture of a momentum analysed He^+ beam again in collision with air in the gas cell ($p \leq 0.08$ mbar). Metastable He ($2^2S_{1/2}$) is Z^4 times more difficult to quench than hydrogen so we applied an additional electric field ($\approx 8 \times 10^5$ $V\ m^{-1}$) inside the gas cell itself, in addition to the weaker field mentioned above. Nevertheless those He^0 atoms created near the exit of the gas cell are subject only to the weaker field. Tests made by switching off

the stronger field showed an increase of about 20% in the electron loss peak in the forward direction. Using data of Horsdal Pedersen *et al* (1980), the 'contamination' of the helium beam by the surviving metastable component is estimated to be as large as 35–40% in the target area. In the worst case, i.e. a fraction of 40% metastable helium, we estimate that our measured doubly differential cross sections ($d^2\sigma/d\Omega_f dE_f$) could be at most 25% larger than for a pure ground state helium beam.

The diameter of the neutral beam for both projectiles is less than 0.7 mm in the target area, where the beam crosses a directed argon gas jet. After traversing the target area the outgoing projectiles are:

(i) either stripped by a thin carbon foil ($20 \mu\text{g cm}^{-2}$) with well known stripping efficiency (Northcliffe and Schilling 1970) and then collected in a biased Faraday cup where they cause an electric current (single mode measurements);

(ii) or charge state analysed by a post collision electric deflection field and then counted by a high count rate (≈ 1 MHz) beam detector (Rinn *et al* 1982) via the induced secondary electron emission from a metal plate (coincidence measurements).

The cylindrical mirror electron spectrometer is similar to that described by Bernardi *et al* (1988). It can be rotated under vacuum and is initially aligned to the precise forward direction ($\Theta_f = 0^\circ \pm 0.25^\circ$) by locating the maximum yield of the electron loss peak. Input and exit apertures were chosen to give an energy resolution consistent with good transmission ($\Delta\Theta_f = 1.67^\circ$, $\Delta E/E = 3 \times 10^{-2}$). The magnetic field of the earth was compensated by three mutually perpendicular pairs of Helmholtz coils but because of uncertainties in the trajectories of very low energy electrons no data below 25 eV are shown. Electron spectra were accumulated in 3 eV steps for single mode and 13 eV for coincidence mode measurements.

The absolute normalization of the singles data was made by measuring the beam current in a shielded Faraday cup. To determine the transmission function and efficiency of the spectrometer at various Θ_f we first measured absolute DDCS for proton impact on argon at 20° , 30° and 50° and normalized the resulting data to the values given by Rudd *et al* (1976). The same experimental conditions were then used for neutral beam impact. For those angles not measured by Rudd *et al* we used a proton beam and measured the signal from the Ar Auger peak at about 200 eV. This peak has been studied by Stolterfoht *et al* (1974) and is believed to be isotropic.

The coincidence data were normalized by counting the number of transmitted projectiles with a given final charge state. Since the efficiency of the particle detector is less than unity it is not possible to obtain the beam current directly from the particle count rate. For H^0 impact the absolute normalization of the coincidence data was achieved by setting maxima of the coincidence data and the singles data to be equal at the top of the electron loss peak, since at this point the contribution from pure target ionization is negligible. Similarly in the case of He^0 the sum of the coincident intensities for outgoing He^+ and He^{2+} was equated to the singles intensity at the top of that singles intensity. Finally, to monitor the stability of the target gas pressure during the experiment a surface barrier detector was used to count the projectiles scattered by the target gas (Rutherford scattering). The uncertainties in the final absolute doubly differential cross sections are due to the normalization procedures, the counting statistics and, especially for helium impact, the uncertain content of metastable components. They are estimated to be less than 80% for both single mode and coincidence experiments. Relative uncertainties are smaller. Near the electron loss peak maximum they are approximately $\pm 15\%$ but they increase up to $\pm 50\%$ for electron energies lower than 50 eV or higher than 500 eV where the count rate is small.

3. Theory

For electron loss in collisions with heavy target atoms the ejected electron is primarily influenced by the target potential. Therefore the electron emission will be described in terms of capture to the target continuum. Within the semiclassical theory the transition amplitude for exciting the projectile electron from the bound state ψ_i^P (with energy ε_i^P) to the target scattering state ψ_f^T (with energy E_f), and the target electrons from the ground state ϕ_i^T (with energy E_i^T) to a final state ϕ_f^T (with energy E_f^T) is approximated by (3.1).

$$a_{fi}^{SI} = -i \int dt \langle \psi_f^T | V_T | \psi_i^P \rangle \quad \phi_f^T = \phi_i^T$$

$$a_{fi}^{DI} = -i \int dt \langle \phi_f^T \psi_f^T | V_{ce} | \phi_i^T \psi_i^P \rangle - i \int dt \langle \phi_f^T \psi_f^T | V_{pe} G_{of} V_T | \phi_i^T \psi_i^P \rangle \quad \phi_f^T \neq \phi_i^T \quad (3.1)$$

$$V_T = V_{eT} + \langle \phi_i^T | V_{ce} | \phi_i^T \rangle.$$

Two processes are distinguished. The projectile electron may scatter elastically on the target atom ($\phi_f^T = \phi_i^T$), the singly inelastic contribution to electron loss. Alternatively it can scatter inelastically on the target leading to target excitation ($\phi_f^T \neq \phi_i^T$), the doubly inelastic contribution to electron loss. For a_{fi}^{SI} the transition is induced by the effective target field V_T consisting of the electron-target nucleus (V_{eT}) and the mean electron-target electron (V_{ce}) interaction. A first-order theory gives a satisfactory description. For a_{fi}^{DI} we have a coherent and an incoherent term. The latter is of second order and describes the incoherent projectile-target ionization due to two subsequent couplings between the projectile electron and the target field (V_T), and the target electrons and the projectile central field (V_{pe}). This field accounts for the presence of passive projectile electrons. The propagation is in the target field, $G_{of} = (i\partial_t - H_T - T_e - V_T + i\varepsilon)^{-1}$ where H_T is the electronic Hamiltonian of the target atom and T_e the kinetic energy of the active projectile electron. The first-order term in a_{fi}^{DI} , describing the coherent projectile-target ionization due to V_{ce} , is small for large emission angles because the electron-electron coupling does not provide the large momenta needed to eject the projectile electron with large energy relative to the projectile. Test calculations within the first-order Born theory for electron loss indicate that for argon targets the coherent ionization is unimportant for angles $> 30^\circ$ and hence only the second-order term in a_{fi}^{DI} will be retained.

Fourier transforming the projectile state Ψ_i^P and using a straight-line path with impact parameter b for the internuclear trajectory $\mathbf{R} = \mathbf{b} + \mathbf{v}t$, where \mathbf{v} is the collision velocity, a_{fi}^{SI} becomes

$$a_{fi}^{SI} = -2\pi i \int d\mathbf{q} \delta(\Delta\varepsilon_{fi} + v^2/2 - \mathbf{q}\mathbf{v}) e^{-i\mathbf{q}\mathbf{b}} \langle \psi_f^T | V_T | \mathbf{q}^T \rangle \varphi_i^P(\mathbf{q} - \mathbf{v}). \quad (3.2)$$

Here $\Delta\varepsilon_{fi} = E_f - \varepsilon_i^P$ is the energy transferred to the projectile electron and $|\mathbf{q}^T\rangle = (2\pi)^{-3/2} \exp(i\mathbf{q}\mathbf{r}_T)$, \mathbf{r}_T being the electron coordinate in the target frame of reference. For the further evaluation of (3.2) the scattering matrix element is replaced by the elastic scattering amplitude

$$\langle \psi_f^T | V_T | \mathbf{q}^T \rangle \approx -\frac{1}{(2\pi)^2} f(q, \theta_{q,k_f}) \quad (3.3)$$

and the peaking of the initial electronic state in momentum space $\varphi_i^P(\mathbf{q} - \mathbf{v})$ at $\mathbf{q} = \mathbf{v}$ is used in (3.3) to replace \mathbf{q} by $q_z \mathbf{e}_z = (\Delta\varepsilon_{fi} + v^2/2) \mathbf{e}_z / v$. The z -direction \mathbf{e}_z is chosen

parallel to \mathbf{v} . As shown in Jakubařa (1980) the singly inelastic part of the loss cross section can then be cast into a product consisting of the cross section $d\sigma_e/d\Omega = |f(\mathbf{q}_z, \Theta_f)|^2$ for elastic electron scattering on the target field and the Compton profile J_i needed to account for the momentum distribution of the initial electronic state

$$\frac{d^2\sigma^{SI}}{dE_f d\Omega_f} = \frac{k_f}{v^2} J_i(\mathbf{q}_z - \mathbf{v}) \frac{d\sigma_e}{d\Omega}(\mathbf{q}_z, \Theta_f). \tag{3.4}$$

Here, Θ_f is the emission angle of the electron and $E_f = k_f^2/2$ with k_f the electronic momentum in the target frame. From (3.4) it is obvious that the cross section peaks near $\mathbf{q}_z = \mathbf{v}$, i.e. near $E_f = v^2/2 + \epsilon_i^P$ and the peak width is determined by J_i . The influence of the target through the scattering cross section $d\sigma_e/d\Omega$ leads to angular dependent variations of the peak position and width. In this context it is very important that the scattering amplitude is calculated from exact target scattering states which are obtained from solving an appropriate Schödinger equation (Jhanwar *et al* 1978).

The incoherent contribution is evaluated by introducing a complete set of eigenstates to $H_T + T_e + V_T$, $\psi_n^T * \phi_n^T$. With this the propagator G_{of} reduces to an energy denominator. Since V_T only couples the states of the projectile electron, while V_{Pe} only affects the target states, orthogonality between ϕ_n^T and ϕ_i^T , and between ψ_f^T and ψ_n^T , can be used to eliminate the sum over intermediate states. Hence we have

$$a_{fi}^{DI} = -i \int dt e^{i(E_f^T + E_f^P)t} \langle \psi_f^T | V_{Pe} | \phi_i^T \rangle \frac{1}{i\partial_t - E_i^T - E_f + i\epsilon} \langle \psi_f^T | V_T | \psi_i^P \rangle e^{-i(E_f^T + \epsilon_i^P)t} \tag{3.5}$$

where the energy phases of the initial and final states have been written explicitly. Next ψ_i^P is transformed into the target frame of reference and the Fourier transform of V_{Pe} and ψ_i^P is introduced. This makes the time integral trivial and we obtain

$$a_{fi}^{DI} = -\frac{i}{\sqrt{2\pi}} \int d\mathbf{q} \delta(\Delta E_{fi}^T + \Delta \epsilon_{fi} + v^2/2 - \mathbf{q}\mathbf{v}) e^{-i\mathbf{q}\mathbf{b}} \int ds \tilde{V}_{Pe}(s) \frac{1}{\Delta E_{fi}^T - s\mathbf{v} + i\epsilon} \times \langle \psi_f^T | V_T | (\mathbf{q} - s)^T \rangle \phi_i^P(\mathbf{q} - s - \mathbf{v}) \langle \phi_f^T | \sum_{n=1}^N e^{i\mathbf{s}\mathbf{r}_n} | \phi_i^T \rangle \tag{3.6}$$

where $\Delta E_{fi}^T = E_f^T - E_i^T$ is the target excitation energy and \tilde{V}_{Pe} is the Fourier transformed projectile central field ($\tilde{V}_{Pe} = -[2/\pi]^{1/2}/s^2$ for H^0 and $-[2/\pi]^{1/2}[2 - \langle \varphi_{1s} | \exp(i\mathbf{s}\mathbf{r}) | \varphi_{1s} \rangle]/s^2$ for He^0). We denote the He^+ ground-state function as φ_{1s}). The structure is similar to (3.2) except for the appearance of the excitation matrix element for the N target electrons. The evaluation of this incoherent doubly inelastic cross section is described in detail in Jakubařa-Amundsen (1992). Basically, similar approximations as for the singly inelastic cross section are applied. The sum over the target final states is evaluated by means of a closure approximation introduced by Hartley and Walters (1987a) which particularly considers target excitation to the continuum. One finds

$$\frac{d^2\sigma^{DI}}{dE_f d\Omega_f} = \frac{8\pi k_f}{v^2} \int_0^\infty \kappa_T^2 d\kappa_T \int_{q_{min}}^\infty q dq S_{in}(k) |M(\mathbf{q})|^2 \frac{\bar{G}(\kappa_T, k)}{\int_0^\infty \kappa_T^2 d\kappa_T \bar{G}(\kappa_T, k)}$$

$$M(\mathbf{q}) = -\frac{1}{2^{5/2}\pi^{3/2}} \int_{-\infty}^\infty ds_z \frac{1}{\Delta E_{fi}^T - s_z v + i\epsilon} f(|\mathbf{q}_z - s_z|, \Theta_f) \int ds_\perp \tilde{V}_{Pe}(s) \phi_i^P(\mathbf{q} - s - \mathbf{v}) \tag{3.7}$$

$$\bar{G}(\kappa_T, k) = \int d\Omega_\kappa \sum_{n=1}^N | \langle \varphi_f^T | e^{i\mathbf{k}\mathbf{r}} | \varphi_n^T \rangle |^2.$$

The target states were taken as Slater determinants composed of single-particle Hartree-Fock states φ_n^T , φ_f^T is a target continuum state with momentum κ_T , $d\Omega_\kappa$ the corresponding solid angle of emission, $\Delta E_{fi}^T = \Delta + \kappa_T^2/2$ where Δ is the target ionization potential and $S_{in}(k)$ with $k = q_\perp + (\Delta E_{fi}^T/v)\mathbf{e}_z$ is the incoherent scattering form factor (Cromer and Mann 1967). The minimum momentum transfer is $q_{\min} = (\Delta E_{fi}^T + \Delta \varepsilon_{fi} + v^2/2)/v$, and $q_\perp^2 = q^2 - q_{\min}^2$. Notice that the quantity $\bar{G}(\kappa_T, k)$, originally introduced by Hartley and Walters (1987a) to ensure completeness of the target states, appears in both the numerator and the denominator of (3.7). Hence the use of hydrogenic 1s states for φ_n^T with a scaled effective charge ($Z_{\text{eff}} = 2.25$ for the Ar valence electrons) does not lead to severe inaccuracies. The advantage of hydrogen-like single-particle projectile and target states is an analytic evaluation of the integrals over $d\mathbf{s}_\perp$ (the \mathbf{s} components perpendicular to \mathbf{v}) and over $d\Omega_\kappa$ (Hartley and Walters 1987a, Jakubaša-Amundsen 1992). In the numerical calculation of the electronic scattering eigenstates the static target potential has been parametrized according to Strand and Bonham (1964), while the parameters of the polarization potential defined in Jakubaša-Amundsen (1992) are taken as $\alpha = 13.333$, $\Delta = 0.58$ and $k_0 = 2$. The choice of Δ as the first ionization threshold and the cutoff parameter k_0 has been made such that the experimental low-energy elastic scattering cross sections $d\sigma_e/d\Omega$ from DuBois and Rudd (1975) are reasonably well reproduced. An inclusion of 30 partial waves in the scattering state for argon provides sufficient accuracy. For He^0 an effective charge of 1.7 and a binding energy 0.91795 have been used. Also, a factor of 2 has been included in the cross section so accounting for the possibility to eject either projectile electron.

4. Results

Absolute DDCS for electron ejection in 0.5 MeV $\text{H}^0 + \text{Ar}$ collisions at emission angles ranging from 30° to 180° are shown in figure 2. Three features are seen in the singles spectra. The large and broad electron loss peak at electron momenta close to the projectile velocity is prominent at all angles. The binary encounter peak at the high momenta $\approx 2v \cos \Theta_f$ is of course visible only at the smaller angles. There is a large signal from low energy electrons. The latter two features are conventionally ascribed to target electrons and it is instructive to compare the signal produced by H^0 with that produced by H^+ , also shown in figure 2. Both projectiles are equally effective in producing the high energy binary encounter electrons since a hard collision is needed so that screening in the H^0 is ineffective, however the long range Coulomb field of H^+ is more effective in producing low energy electrons. The argon LMM Auger peak at about 200 eV, clearly visible during proton impact, is completely submerged in the electron loss peak from H^0 which now stands more than an order of magnitude above it.

When H^0 is used as the projectile and electrons are counted in coincidence with outgoing H^+ the signal near the top of the loss peak is essentially the same as that from the non-coincident run, because in this region all electrons originate from the projectile. However, as we proceed to the low energy side of the loss peak or to the binary peak region, the coincidence data progressively fall below the singles data. The difference between the singles and the coincidence data is due to 'pure' target ionization, leaving the projectile unaffected. In the coincidence experiments, the final charge state of the target was not measured. Therefore, the origin of the detected electrons is twofold: they may be projectile electrons leaving the target inert or excited;

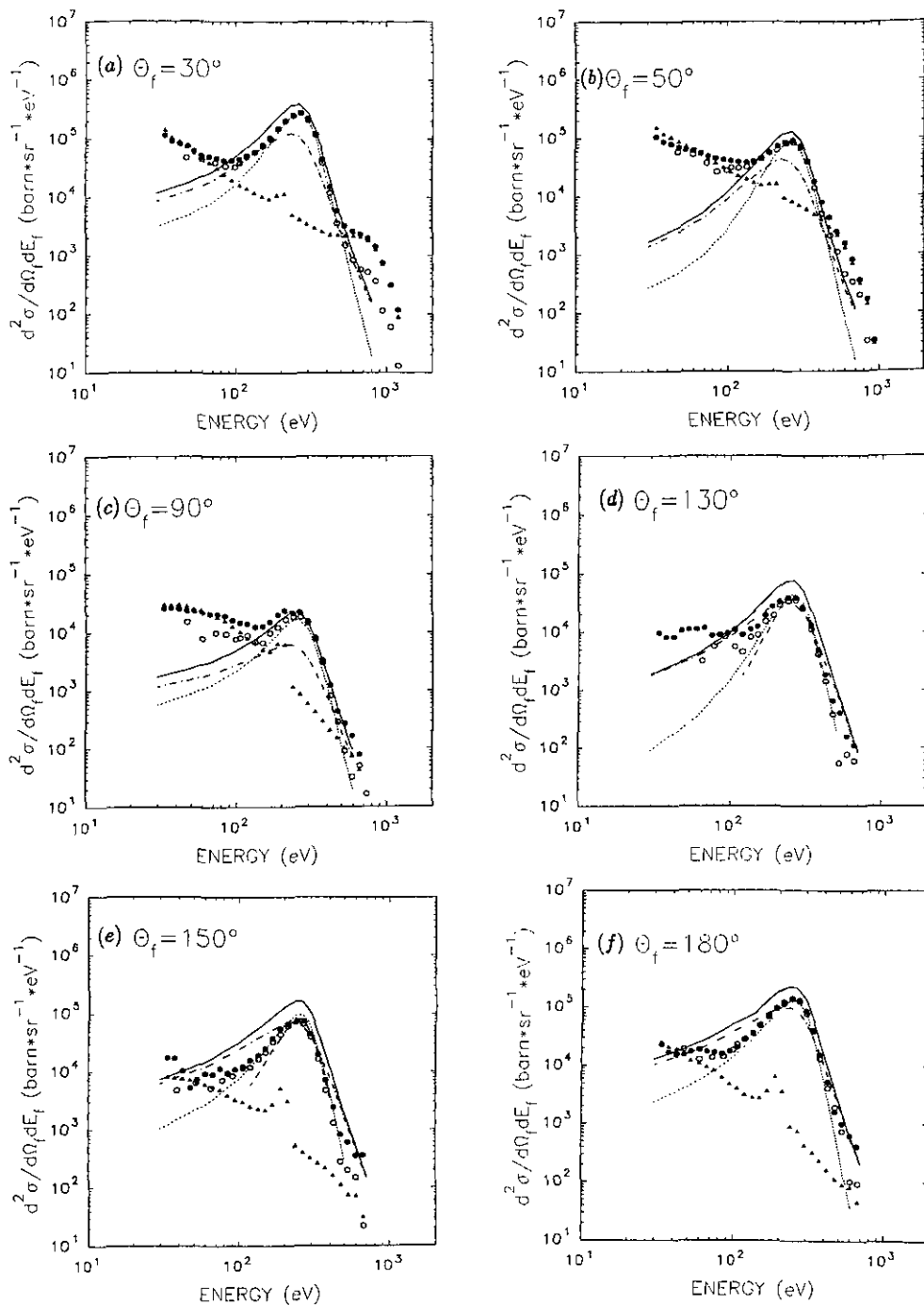


Figure 2. Absolute doubly differential cross sections for 0.5 MeV H^0 and H^+ impact on Ar. Experiment: \blacktriangle , single mode H^+ ; \bullet , single mode H^0 ; \circ , loss coincident $H^0 \rightarrow H^+$. Our theory: ---, singly inelastic; - · -, doubly inelastic; —, sum; · · ·, SI theory of Wang *et al* (1991). The number of experimental data points actually shown has been reduced to avoid overcrowding the figure.

the latter process being the simultaneous projectile-target ionization identified by DuBois and Manson (1986). However, the electrons may also be target electrons with the projectile being simultaneously ionized, preferably at very small E_f and in the binary peak region.

The theoretical curves from section 3 are also shown in figure 2. It is seen that for all angles the data near the loss peak maxima are well described by just the singly inelastic part of the EIA theory. However on the low-energy side this theory drops off too fast. In principle this could be due to the approximations made in the step from (3.2) to (3.4). Wang *et al* (1991) have avoided these particular approximations but their s_1 cross sections at the two angles 130° and 150° are even further below our data on the low energy side. Inclusion of the D_1 simultaneous projectile-target ionization enhances the cross section considerably, particularly on this low energy side of the loss peak. This confirms the conjecture (Heil *et al* 1991a) that the doubly inelastic events play a significant role in the differential electron spectra. The theoretical intensity at small E_f still falls far below the coincidence data. Part of this deficiency may be attributed to the fact that one cannot distinguish experimentally between target continuum electrons (Kövér *et al* 1989) and projectile electrons even in our coincidence arrangement. The presence of target continuum electrons leads to a modification of the spectrum which is not accounted for in the theory. We point out that a calculation of the D_1 part of the process again avoiding the approximations corollary to (3.2)–(3.4) will presumably reduce the D_1 contribution just as it did for the s_1 contribution, so this is of no help. At $\Theta_f = 30^\circ$ inclusion of the coherent part of the D_1 contribution may double this part of theory but this is still not sufficient to account for the measured intensity below 80 eV. In contrast adding the incoherent part of the D_1 channel to the s_1 channel raises the theoretical cross section above the experimental value near the maximum of the electron loss peak and this overprediction becomes progressively more serious as Θ_f increases towards 180° . The consequences of this overprediction by the theory are clearly seen in the singly differential cross section (SDCS) shown in figure 3 where we compare our recent data (integrated over the energy range 140–370 eV) to that of Duncan and Menendez (1979), our present theory, and the theory of Hartley and Walters (1987b). The new data are substantially different from the earlier (1979) results. This may reflect improvements in electron spectroscopy over the last decade but a further independent measurement is clearly desirable. We know conclusively from the coincidence measurements that D_1 processes do play an important part in the electron ejection yet we see that an EIA theory which ignores them and considers only s_1 processes actually gives a better fit to our data at $\Theta_f \geq 120^\circ$. This is of course spurious.

Passing now to our results for He^0 incident on Ar we show DDCS for three ejection angles in figure 4. The same three general features exhibited in figure 2 are present and again we believe there is a contribution to the signal which must arise from D_1 events. Additionally in the $\Theta_f = 30^\circ$ results it is just possible to see that the coincidence data from He^0 becoming doubly stripped to He^{2+} are broader than those for single electron loss. This illustrates the influence of the Compton profile J_i on the measured spectra referred to in section 3. In making a comparison with theory we see that the small discrepancies present in the hydrogen data in figure 2 have become severe for the helium projectile. Inclusion of the D_1 term results in an overprediction of the DDCS which is now quite clear even at $\Theta_f = 30^\circ$ and again becomes progressively more serious at higher angles. Now, even the s_1 process alone overestimates the magnitude of the cross section for the two backward angles, giving reasonable predictions only at 30° .

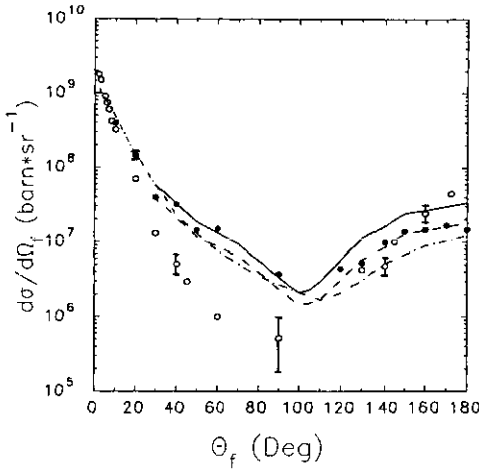


Figure 3. Absolute singly differential cross sections for 0.5 MeV H^0 impact on Ar. Experiment: ●, our single mode data; ○, data of Duncan and Menendez (1979). Our theory: ---, singly inelastic; —, sum of singly and doubly inelastic. - · -, SI + first-order DI theory of Hartley and Walters (1987b).

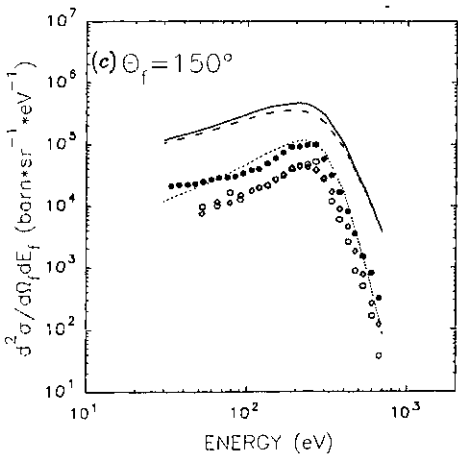
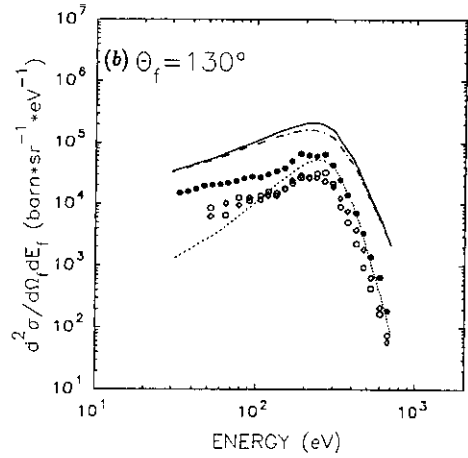
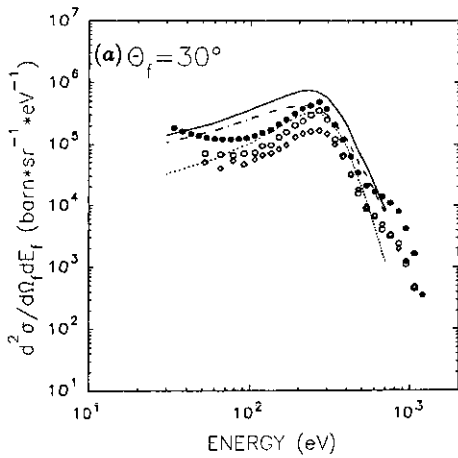


Figure 4. Absolute doubly differential cross sections for 0.5 MeV $u^{-1} He^0$ impact on Ar. Experiment: ●, single mode He^0 ; ○, loss coincident $He^0 \rightarrow He^+$; ◇, loss coincident $He^0 \rightarrow He^{2+}$. Our theory: ---, singly inelastic; - · -, doubly inelastic; —, sum. The number of experimental data points actually shown has been reduced to avoid overcrowding the figure.

5. Conclusions

The use of coincidence techniques to isolate the separate processes contributing to electron ejection during ion-atom collisions involving structured projectiles had previously shown the importance of simultaneous projectile-target ionization. Absolute DDCS are now available for the simple projectiles H^0 , He^+ , He^0 , all of which have reasonably well characterized wavefunctions, incident on helium and argon targets. The experimental evidence for the simultaneous process is now so well established that any theory which describes only the s_1 channel cannot in principle be correct even if it predicts the correct numerical values. Inclusion of both coherent and incoherent parts of the D_1 channel within the EIA has yet to be attempted. A calculation of the electron loss for H^0 incident on the light target helium using the second-order Born approximation (Jakubaša-Amundsen 1992) has shown that inclusion of both D_1 contributions substantially improves the agreement between theory and experiment for ejection at 30° (Heil *et al* 1991b). For the larger emission angles and energies, the incoherent part of D_1 is dominant and hence consideration of just this part should be sufficient. For the heavier argon target, the EIA (including only the incoherent D_1 channel) leads to some overprediction by the theory, at least for high ejection angles.

When He^+ (DuBois and Manson 1990) and He^0 projectiles are incident on helium the agreement between theory and experiment remains reasonable but when the theory is applied to an argon target large discrepancies arise because the incoherent D_1 contribution adds considerably to an s_1 channel which itself fully accounts for (at 30°) or even overestimates (at backward angles) the observed electron loss peak. The source of these discrepancies is probably the use of a truncated perturbation series (the second-order Born type EIA theory) which becomes more invalid the stronger the perturbing field (i.e. the heavier the target) at the comparatively low impact energy used in the present experiments. Calculating to higher order than second Born is very intricate, so the way out of this difficulty remains a challenge but it must be resolved if electron loss from the highly structured heavy ions now available is to be understood.

Acknowledgments

Supported by BMFT/Bonn under contract number 06 OF 110/Ti 476 Gr and GSI-Darmstadt under project number 45/92. We should like to thank the DAAD and British Council for financial support during this collaboration.

References

- Bates D R and Griffing G 1954 *Proc. Phys. Soc. A* **67** 663-8
- Bernardi G, Suarez S, Focke P and Meckbach W 1988 *Nucl. Instrum. Methods B* **33** 321-5
- Bethe H 1930 *Ann. Phys., Lpz.* **5** 325-400
- Bethe H A and Salpeter E E 1957 *Quantum Mechanics of One and Two Electron Atoms* (Berlin: Springer)
- Bohr N 1948 *K Dansk Vidensk. Selsk. Mat. Fys. Meddr.* **18** No 8
- Burch D, Wieman H and Ingalls W B 1973 *Phys. Rev. Lett.* **30** 823-6
- Cromer D T and Mann J B 1967 *J. Chem. Phys.* **47** 1892
- Dettmann K, Harrison K G and Lucas M W 1974 *J. Phys. B: At. Mol. Phys.* **7** 269-87
- Dr Pepper F and Briggs J S 1976 *J. Phys. B: At. Mol. Phys.* **9** 2063-71
- DuBois R D and Manson S T 1986 *Phys. Rev. Lett.* **57** 1130-2
- 1990 *Phys. Rev. A* **42** 1222-30

- DuBois R D and Rudd M E 1975 *J. Phys. B: At. Mol. Phys.* **8** 1474-83
- Duncan M M and Menendez M G 1979 *Phys. Rev. A* **19** 49-54
- 1981 *Phys. Rev. A* **23** 1085-88
- Feagin J M, Briggs J S and Reeves T M 1984 *J. Phys. B: At. Mol. Phys.* **17** 1057-68
- Hartley H M and Walters H R 1987a *J. Phys. B: At. Mol. Phys.* **20** 1983-2003
- 1987b *J. Phys. B: At. Mol. Phys.* **20** 3811-31
- Heil O, DuBois R D, Maier R, Kuzel M and Groeneveld K-O 1991a *Z. Phys. D* **21** 235-9
- 1991b *Phys. Rev. A* **45**
- Heil O, Kuzel M, Maier R, Trabold H, Lucas M W, Berényi D and Groeneveld K O 1991c *Proc. 17th Int. Conf. on Physics of Electronic and Atomic Collisions* 552
- Horsdal Pedersen E, Heinemeier J, Larsen L and Mikkelsen J V 1980 *J. Phys. B: At. Mol. Phys.* **13** 1167-83
- Jakubaša D H 1980 *J. Phys. B: At. Mol. Phys.* **13** 2099-108
- Jakubaša-Amundsen D H 1990 *J. Phys. B: At. Mol. Opt. Phys.* **23** 3335-51
- 1992 *Z. Phys. D* **22**
- Jhanwar B L, Khare S P and Kumar Ashok Jr 1978 *J. Phys. B: At. Mol. Phys.* **11** 887-94
- Kövér Á, Szabó Gy, Gulyás L, Tökési K, Berényi D, Heil O and Groeneveld K-O 1988 *J. Phys. B: At. Mol. Opt. Phys.* **21** 3231-41
- Kövér Á, Sarkadi L, Palinkas J, Berényi D, Szabó Gy, Vajnai T, Heil O, Groeneveld K O, Gibbons J and Sellin I A 1989 *J. Phys. B: At. Mol. Opt. Phys.* **22** 1595-602
- Macek J 1970 *Phys. Rev. A* **1** 235-41
- Merzbacher E and Lewis H W 1958 *Handbuch der Physik* **34** 166-92
- Northcliffe L C and Schilling R F 1970 *Nucl. Data Tables A* **7** 233-463
- Rinn K, Müller A, Eichenauer H and Salzborn E 1982 *Rev. Sci. Instrum.* **53** 829-37
- Rudd M E and Macek J H 1972 *Case Studies in Atomic Physics* vol 3, ed E W McDaniel and M R C McDowell (Amsterdam: North-Holland) pp 49-136
- Rudd M E, Toburen L H and Stolterfoht N 1976 *At. Data Nucl. Data Tables* **23** 405-42
- Stolterfoht N, Schneider D and Ziem P 1974 *Phys. Rev. A* **10** 81-91
- Strand T G and Bonham R A 1964 *J. Chem. Phys. B* **20** 1686
- Strong R and Lucas M W 1977 *Phys. Rev. Lett.* **39** 1349-52
- Thomas L H 1927 *Proc. Camb. Phil. Soc.* **23** 713-6
- Wang J, Reinhold C O and Burgdörfer J 1991 *Phys. Rev. A* **44** 7243-51
- 1992 *Phys. Rev. A* **45**